

OPTIMAL VECTOR SEQUENCE WITH SPACE VECTOR MODULATION IN DIRECT TORQUE CONTROL OF INDUCTION MOTOR

¹JYOTHILAL NAYAK BHAROTHU

²V GOPILATHA

¹Associate professor of Electrical & Electronics Engineering,

²Assistant professor of Electrical & Electronics Engineering,

Sri Vasavi Institute of Engineering & Technology, Nandamuru, A.P.; India

ABSTRACT

In this paper effective direct torques control (DTC) for a 5-phase induction motor with sinusoidal distributed windings is developed. First by coordinate transformation, the converter/motor models are represented by two independent equivalent d-q circuit models; and the 5-phase VSI input are decoupled into the torque producing and non-torque producing harmonics sets. Then with the torque production component of the induction motor model, the space vector modulation (SVM) can be applied to the five-phase induction motor DTC control, resulting in considerable torque ripple reduction over the lookup table method. Based on the decoupled system model, the current distortion issue due to lack of back EMF for certain harmonics is analyzed. Two equally effective SVM schemes with the harmonic cancellation effect are introduced to solve this problem. To analyze the DTC control torque ripple, an insightful perspective (also applicable to 3-phase analysis) is introduced to predict the torque ripple pattern evolution with changing motor speed and stator flux angular position. Therefore the switching sequence for lowest torque ripple can be determined and re-arranged online. Finally, with the overall optimal switching scheme adopted.

Key words: DTC, SVM, INDUCTION MOTOR, EMF DISTRIBUTION, MAT LAB etc

1.0 Introduction

Direct torque control (DTC) has been gaining more popularity since its introduction due to its exceptional dynamic response and less dependence on machine parameters. It has been applied to the multi-phase motor, in which DTC with a lookup table is used to control 5-phase induction motor and a PMSM with concentrated stator windings. Due to the abundance of voltage vectors in the 5-phase drive system, steady-state torque ripple performance showed considerable improvement over comparable 3-phase drives. The first contribution of this paper is to replace the lookup table DTC with the DTC space vector modulation in the 5-phase IM drive.

This type of control further reduces the torque ripple because it can produce the voltage reference which accurately compensates the differences between the commanded torque/flux values and their actual values from measurement and estimation. The look up table DTC, uses alternatively "forward" and "backward" active vectors to bring the flux and torque within the hysteresis band. For the lookup table DTC, the analog hysteresis control has the issue of varying switching frequency but its torque ripple can be controlled by setting the hysteresis band; the digital hysteresis implementation has a fixed switching frequency, but the larger torque ripple become an issue. Moreover, it is shown in the paper that in 5-phase motors with sinusoidally distributed stator windings, the absence of back EMF for non-torque-producing harmonics (mostly the 3rd harmonic) will result in considerable harmonic current, if the modulation scheme can't completely cancel out such voltage harmonics using the VSI inverter.

This causes deformation of the phase current and extra copper losses (while not causing torque pulsation). For sinusoidal results, the lookup table DTC and even the DTC using SVM (with one pair of closest vectors plus the zero-vector) can't be used in a sinusoidal wound 5-phase motor. At least two pairs of voltage vectors with the zero-vector are required for the harmonic free operation. Two such SVM schemes are introduced in this paper. The last part of this paper systematically addresses several concepts such as how to evaluate if certain switching sequence (vector sequence) will achieve minimal torque ripple, analytically predicting the torque ripple pattern without simulation, and the torque ripple shape as motor speed change.

1.1 Overview of Induction Motor:

The induction motors have more advantages over the rest of motors. The main advantage is that induction motors do not require an electrical connection between the stationary and the rotating parts of the motor. Therefore, they do not need any mechanical commutator (brushes), leading to the fact that they are maintenance free motors.

Besides, induction motors also have low weight and inertia, high efficiency and a high overload capability. Therefore, they are cheaper and more robust, and less prone to any failure at high speeds. Furthermore, the motor can work in explosive environments because no sparks are produced.

Taking into account all of the advantages outlined above, the induction motors must be considered as the perfect electrical to mechanical energy converter. However, mechanical energy is more than often required at variable speeds, where the speed control system is not an insignificant matter.

The only effective way of producing an infinitely variable induction motor speed drive is to supply the induction motor with three phase voltages of variable frequency and variable amplitude. A variable frequency is required

because the rotor speed depends on the speed of the rotating magnetic field provided by the stator. A variable voltage is required because the motor impedance reduces at the low frequencies and consequently the current has to be limited by means of reducing the supply voltages. Another alternative method of speed control can be realized by means of a wound rotor induction motor, where the rotor winding ends are brought out to slip rings. However, this method obviously removes most of the advantages of the induction motors and it also introduces additional losses. By connecting resistors or reactance in series with the stator windings of the induction motors, poor performance is achieved. Historically, several general controllers have been developed.

1.2 Scalar controllers:

Despite the fact that “Voltage-Frequency” (V/f) is simplest controller, it is the most widespread, being in the majority of the industrial applications. It is known as a scalar control and acts by imposing a constant relation between voltage and frequency. The structure is simple and it is normally used without speed feedback. However, this controller does not achieve a good accuracy in both speed and torque responses, mainly regarding to the fact that the stator flux and torque are not directly controlled. Even though, as long as the parameters are identified, the accuracy in the speed can be 2%, and the dynamic response can be approximately around 50ms.

1.3 Vector Controllers:

In these types of controller, there are control loops for controlling both the torque and the flux. The most widespread controllers of this type are the ones that use vector transform such as either Park or Ku. Its accuracy can reach values such as 0.5% regarding the speed and 2% regarding the torque, even when at stand still. The main disadvantages are the huge computational capability required and the compulsory good identification of the motor parameters.

According to these types of controllers, there are control loops for controlling both the torque and the flux. The most widespread controllers are the ones that use vector transform such as either Park or Ku. Its accuracy can reach values such as 0.5% regarding the speed and 2% regarding the torque, even in stand still. The main disadvantages are the huge computational capability required and the compulsory good identification of motor parameters.

1.4. Field Acceleration Method:

This method is based on the maintaining the amplitude and the phase of the stator current constant, whilst avoiding electromagnetic transients. Therefore, the equations can be simplified saving the vector transformation, which occurs in the vector controllers.

This technique has achieved some computation reduction, thus overcoming the main problem with vector controllers and allowing this method to become an important alternative to vector controllers. The equation used in this method can be simplified avoiding the vector transformation. It is achieved some computational reduction, overcoming the main problem in the vector controllers and then becoming an important alternative for the vector controllers.

DTC is said to be one of the future ways of controlling the induction machine in four quadrants. In the DTC, it is possible to control directly the stator flux and the torque by selecting the appropriate inverter state. This method still required further research in order to improve the motor's performance, as well as achieve a better behaviour regarding environment compatibility (Electro Magnetic Interference and Energy), that is desired nowadays for all industrial applications.

1.5 Induction Motor Controllers:

There are too many different ways to drive an induction motor. The main differences between them are the motor's performance and the viability and cost in its real implementation. Despite the fact that “Voltage/Frequency” (V/Hz) is the simplest controller, it is the most widespread, being in the majority of the industrial applications. It is known as a scalar control and acts imposing a constant relation between voltage and frequency. The structure is very simple and it is normally used without speed feedback. However, this controller does not achieve a good accuracy in both speed and torque response mainly due to the fact that the stator flux and the torque are not directly controlled. Even though, as long as the parameters are identified, the accuracy in the speed can be 2% and dynamic response can be approximately around 50ms.

1.6 Direct Torque Control

In direct torque control (DTC), it is possible to control directly the stator flux and the torque by selecting the appropriate inverter switching state. Its main features are as follows

Direct torque control and direct stator flux control. Indirect control of stator currents and voltages., Approximately sinusoidal stator fluxes and stator currents, High dynamic performance even at locked rotor., This method presents the following advantages:., Absences of co-ordinates transform., Absences of mechanical transducers., Current regulators, PWM pulse generation, PI control of flux and torque and co-ordinate transformation are not required., Very simple control scheme and low computation time., Reduced parameters sensitivity., Very good dynamic properties.,

Although, some disadvantages are present:

High torque ripples and current distortions, Low switching frequency of transistors with relation to computation time, Constant error between reference and real torque

2. ROTATING TRANSFORMATION:

The DQ transformation is a transformation of coordinates from the three-phase stationary coordinate system to the dq rotating coordinate system. This transformation is made in two steps:

1. a transformation from the three-phase stationary coordinate system to the two-phase, so-called $\alpha\beta$, stationary coordinate system and
2. a transformation from the $\alpha\beta$ stationary coordinate system to the dq rotating coordinate system.

These steps are shown in Figure 2.1. A representation of a vector in any n-dimensional space is accomplished through the product of a transpose n-dimensional vector of coordinate units and a vector representation of the vector, whose elements are corresponding projections on each coordinate axis, normalized by their unit values. In three phase space, it looks like this:

$$X_{abc} = \begin{bmatrix} a_u & b_u & c_u \end{bmatrix} \begin{bmatrix} x_a \\ x_b \\ x_c \end{bmatrix} \quad 2.1$$

Assuming a balanced three-phase system ($x_0 = 0$), a three-phase vector representation transforms to dq vector representation (zero-axis component is 0) through the transformation matrix T, defined as:

$$T = \frac{2}{3} \begin{bmatrix} \cos(\omega t) & \cos(\omega t - \frac{2}{3}\pi) & \cos(\omega t + \frac{2}{3}\pi) \\ -\sin(\omega t) & -\sin(\omega t - \frac{2}{3}\pi) & -\sin(\omega t + \frac{2}{3}\pi) \end{bmatrix} \quad 2.2$$

In other words, the transformation from X (dq rotating coordinates), called Park's transformation, is obtained through the multiplication of the vector X_{abc} by the matrix T:

$$X_{abc} = \begin{bmatrix} X_a \\ X_b \\ X_c \end{bmatrix} \quad 2.3$$

$$X_{dq} = \begin{bmatrix} X_d \\ X_q \end{bmatrix} \quad 2.4$$

$$\begin{bmatrix} \alpha_u & \beta_u & o_u \end{bmatrix} = \begin{bmatrix} a_u & b_u & c_u \end{bmatrix} \frac{2}{3} \begin{bmatrix} 1 & 0 & \frac{1}{2} \\ -\frac{1}{2} & \frac{\sqrt{3}}{2} & \frac{1}{2} \\ -\frac{1}{2} & -\frac{\sqrt{3}}{2} & \frac{1}{2} \end{bmatrix} \quad \begin{bmatrix} d_u & q_u & o_u \end{bmatrix} = \begin{bmatrix} \alpha_u & \beta_u & o_u \end{bmatrix} \begin{bmatrix} \cos\theta & -\sin\theta & 0 \\ \sin\theta & \cos\theta & 0 \\ 0 & 0 & 1 \end{bmatrix} \quad 2.5$$

$$\begin{bmatrix} d_u & q_u & o_u \end{bmatrix} = \begin{bmatrix} a_u & b_u & c_u \end{bmatrix} \frac{2}{3} \begin{bmatrix} \cos\theta & -\sin\theta & \frac{1}{2} \\ \cos(\theta - \frac{2\pi}{3}) & -\sin(\theta - \frac{2\pi}{3}) & \frac{1}{2} \\ \cos(\theta + \frac{2\pi}{3}) & -\sin(\theta + \frac{2\pi}{3}) & \frac{1}{2} \end{bmatrix} \quad 2.6$$

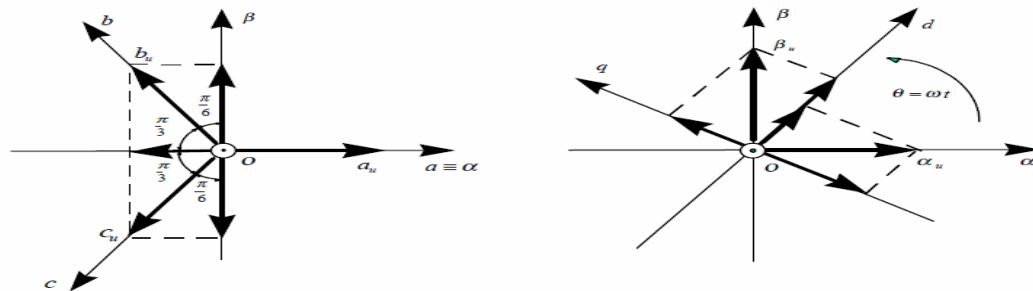


Figure 2.1. Park's transformation from three-phase to rotating dq0 coordinate system

$$X_{dq} = TX_{abc} \quad 2.7$$

The inverse transformation matrix (from dq to abc) is defined as:

$$T' = \begin{bmatrix} \cos(\omega t) & -\sin(\omega t) \\ \cos(\omega t - \frac{2}{3}\pi) & -\sin(\omega t - \frac{2}{3}\pi) \\ \cos(\omega t + \frac{2}{3}\pi) & -\sin(\omega t + \frac{2}{3}\pi) \end{bmatrix} \quad 2.8$$

The inverse transformation is calculated as

$$X_{abc} = T' X_{dq} \quad 2.9$$

2.1. Dynamic d-q Model:

The following assumptions are made to derive the dynamic model:

- (i) uniform air gap;
- (ii) balanced rotor and stator windings, with sinusoidal distributed mmf;
- (iii) inductance vs. rotor position in sinusoidal; and
- (iv) Saturation and parameter changes are neglected

The dynamic performance of an ac machine is somewhat complex because the three-phase rotor windings move with respect to the three-phase stator windings as shown in Figure 2.2a.

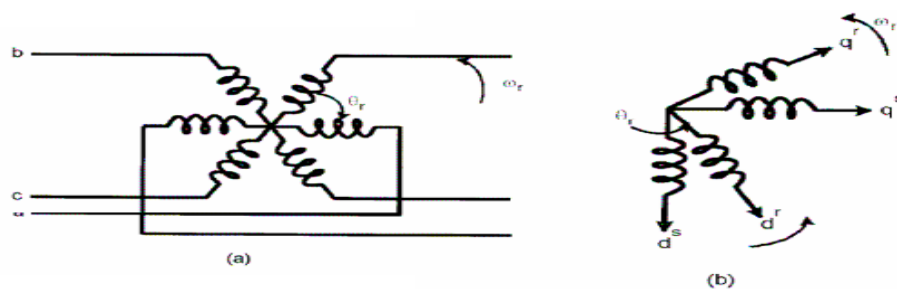


Figure 2.2 (a) Coupling effect in three-phase stator and rotor windings of motor,
(b) Equivalent two-phase machine

Basically, it can be looked on as a transformer with a moving secondary, where the coupling coefficients between the stator and rotor phases change continuously with the change of rotor position θ_r , correspond to rotor direct and quadrature axes. The machine model can be described by differential equations with time-varying mutual inductances, but such a model tends to be very complex. Note that a three-phase machine can be represented by an equivalent two-phase machine as shown in Figure 2.2b, where $d^s \sim q^s$ correspond to stator direct and quadrature axes, and $d^r \sim q^r$.

Although it is somewhat simple, the problem of time-varying parameters still remains. R.H. Park, in the 1920s, proposed a new theory of electric machine analysis to solve this problem. He formulated a change of variables which, in effect, replaced the variables (voltages, currents and flux linkages) associated with the stator windings

of a synchronous machine with variables associated with fictitious windings rotating with the rotor at synchronous speed. Essentially, the transformed or referred, the stator variables to a synchronously rotating reference frame fixed in the rotor. With such a transformation (called Park's transformation), he showed that all the time-varying inductances that occur due to an electric circuit in relative motion and electric circuits with varying magnetic reluctances can be eliminated. Later, in the 1930s, H. C. Stanley showed that time-varying inductances in the voltage equations of an induction machine due to electric circuits in relative motion can be eliminated by transforming the rotor variables to variables associated with fictitious stationary windings. In this case, the rotor variables are transformed to a stationary reference frame fixed on the stator. Later, G. Kron proposed a transformation of both stator and rotor variables to a synchronously rotating reference frame that moves with the rotating magnetic field. D. S. Brereton proposed a transformation of stator variables to a rotating reference frame that is fixed on the rotor. In fact, it was shown later by Krause and Thomas that time-varying inductances can be eliminated by referring the stator and rotor variables to a common reference frame which may rotate at any speed (arbitrary reference frame).

2.2. Axes Transformation:

In order to reduce the expressions of the induction motor equation voltages, three phase to two-phase transformation will be applied. Physically, it can be understood as transforming the three windings of the induction motor to just two windings, as it in the is shown in the figure (2.3)

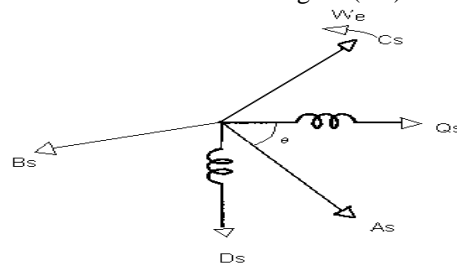


Figure 2.3. Schematic of the equivalence physical transformation

In the symmetrical three-phase machine, the direct and the quadrature-axis stator magnitudes are fictitious. The equivalencies with these direct (d) and quadrature (q) magnitudes with the magnitudes per phase are as follows

$$\begin{bmatrix} V_{as} \\ V_{bs} \\ V_{cs} \end{bmatrix} = \begin{bmatrix} \cos \theta & \sin \theta & 1 \\ \cos(\theta - 120) & \sin(\theta - 120) & 1 \\ \cos(\theta + 120) & \sin(\theta + 120) & 1 \end{bmatrix} \begin{bmatrix} V_{qs}^s \\ V_{ds}^s \\ V_{os}^s \end{bmatrix} \quad 2.10$$

The corresponding inverse relation is:

$$\begin{bmatrix} V_{qs}^s \\ V_{ds}^s \\ V_{os}^s \end{bmatrix} = \frac{2}{3} \begin{bmatrix} \cos \theta & \cos(\theta - 120) & \cos(\theta + 120) \\ \sin \theta & \sin(\theta - 120) & \sin(\theta + 120) \\ 0.5 & 0.5 & 0.5 \end{bmatrix} \begin{bmatrix} V_{as} \\ V_{bs} \\ V_{cs} \end{bmatrix} \quad 2.11$$

Where V_{os}^s is added as the zero sequence component, which may or may not be present. We have considered voltage as the variable. It is assumed that the d^s-q^s axes are oriented at θ angle as shown in the figure (3.2). The current and the flux linkages can be transformed by similar equations. It is convenient to set $\theta = 0$ so that q^s axis is aligned with the as axis. Ignoring the zero sequence component, the transformation relations can be simplified.

$$V_{as} = V_{qs}^s \quad 2.12$$

$$V_{bs} = -\frac{1}{2}V_{qs}^s - \frac{\sqrt{3}}{2}V_{ds}^s \quad 2.13$$

$$V_{cs} = -\frac{1}{2}V_{qs}^s + \frac{\sqrt{3}}{2}V_{ds}^s \quad 2.14$$

and inversely

$$V_{qs}^s = \frac{2}{3}V_{as} - \frac{1}{3}V_{bs} - \frac{1}{3}V_{cs} = V_{as} \quad 2.15$$

$$V_{ds}^s = -\frac{1}{\sqrt{3}}V_{bs} + \frac{1}{\sqrt{3}}V_{cs} \quad 2.16$$

Figure (2.4) shows the arbitrary rotating reference frame $d^a - q^a$ axes, which rotate at arbitrary speed ω_a with respect to $d^s - q^s$ axes and the angle $\theta_a = \omega_a t$. The two phase $d^s - q^s$ axes windings are transformed into the hypothetical windings mounted on the $d^a - q^a$ axes. The voltages on the $d^s - q^s$ axes can be converted (or resolved) into the $d^a - q^a$ frame as follows.

$$V_{qs} = V_{qs}^s \cos \theta_a - V_{ds}^s \sin \theta_a \quad 2.17$$

$$V_{ds} = V_{qs}^s \sin \theta_a + V_{ds}^s \cos \theta_a \quad 2.18$$

and inversely

$$V_{qs}^s = V_{qs} \cos \theta_a + V_{ds} \sin \theta_a \quad 2.19$$

$$V_{ds}^s = -V_{qs} \sin \theta_a + V_{ds} \cos \theta_a \quad 2.20$$

Here V_{qs} and V_{ds} are voltages transformed on to arbitrary reference frame.

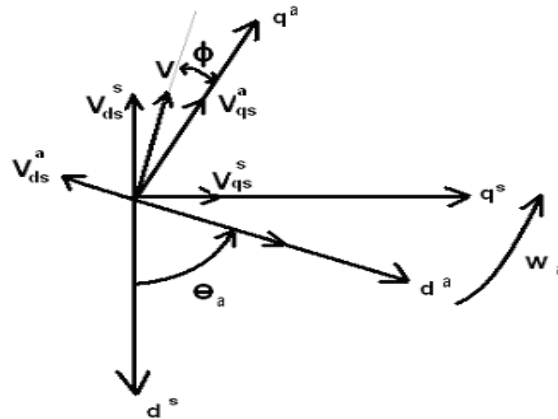


Figure 2.4. stationary reference frame to arbitrary reference frame Transformation

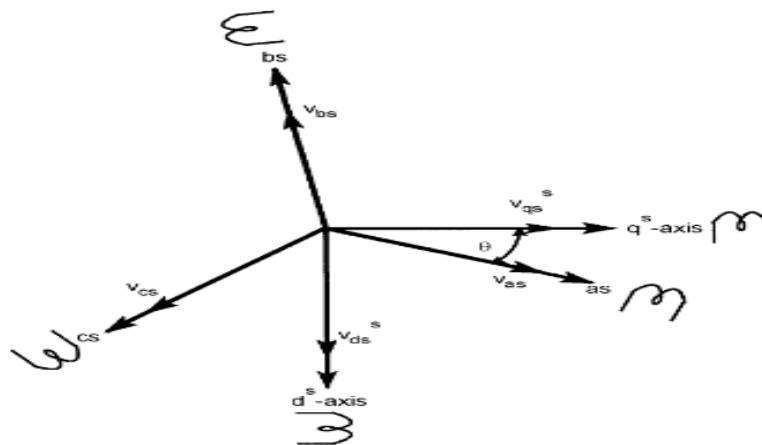


Figure 2.5 Stationary frame a~b~c to $d^s - q^s$ axes transformation

2.3. Space Vector Modulation Basic Principles:

The space vector modulation (SVM) basic principles are shown in Figure 2.6. A classical sinusoidal modulation limits the phase duty cycle signal to the inner circle. The space vector modulation schemes extend this limit to the hexagon by injecting the signal third harmonic. The result is about 10% ($2/1.73 \times 100\%$) higher phase voltage signal at the inverter output. The PWM modulation chops alternatively two adjacent phase voltage and zero voltage signals in a certain pattern producing the switching impulses for the inverter S_a , S_b and S_c . Various

SVM modulation schemes have been proposed in literature and some recent analyzes show that there is a trade-off between the switching losses and the harmonic content, so-called THD, produced by the SVM modulation.

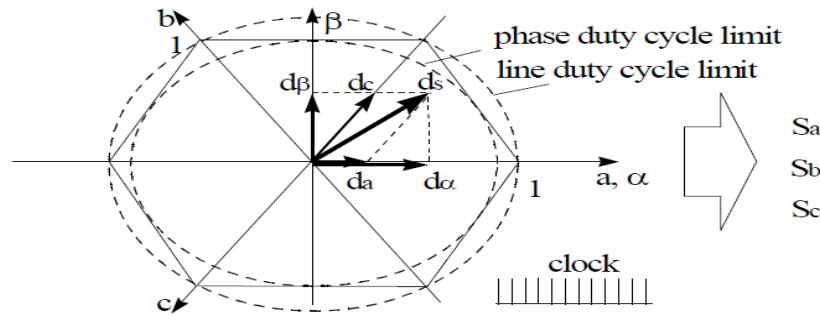


Figure 2.6 Space Vector Modulation Basic Principle

2.3a. Space Vector Modulation:

Space vector modulation is a PWM control algorithm for multi-phase AC generation, in which the reference signal is sampled regularly; after each sample, non-zero active switching vectors adjacent to the reference vector and one or more of the zero switching vectors are selected for the appropriate fraction of the sampling period in order to synthesize the reference signal as the average of the used vectors.

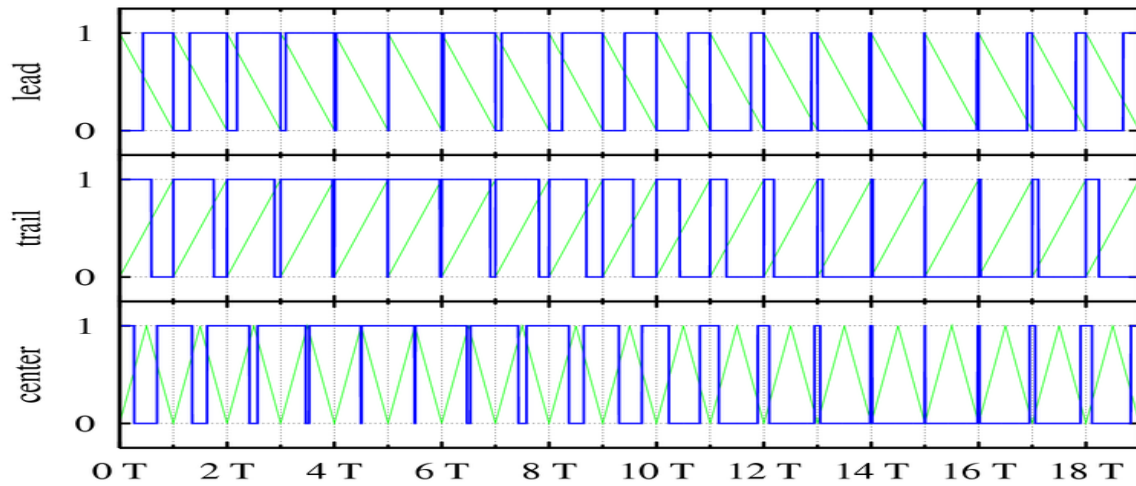


Figure 2.7 Space Vector Modulation Waveforms

2.3b. Direct Torque Control (DTC):

Direct torque control is a method used to control AC motors. It is closely related with the delta modulation (see above). Motor torque and magnetic flux are estimated and these are controlled to stay within their hysteresis bands by turning on new combination of the device's semiconductor switches each time either of the signal tries to deviate out of the band.

2.3c. Time Proportioning:

Many digital circuits can generate PWM signals (e.g. many microcontrollers have PWM outputs). They normally use a counter that increments periodically (it is connected directly or indirectly to the clock of the circuit) and is reset at the end of every period of the PWM. When the counter value is more than the reference value, the PWM output changes state from high to low (or low to high). This technique is referred to as time proportioning, particularly as time-proportioning control – which proportion of a fixed cycle time is spent in the high state. The incremented and periodically reset counter is the discrete version of the intersecting method's sawtooth. The analog comparator of the intersecting method becomes a simple integer comparison between the current counter value and the digital (possibly digitized) reference value. The duty cycle can only be varied in discrete steps, as a function of the counter resolution. However, a high-resolution counter can provide quite satisfactory performance.

Three types of PWM signals (blue): leading edge modulation (top), trailing edge modulation (middle) and centered pulses (both edges are modulated, bottom). The green lines are the sawtooth waveform (first and second cases) and a triangle waveform (third case) used to generate the PWM waveforms using the intersective method.

Three types of pulse-width modulation (PWM) are possible:

1. The pulse center may be fixed in the center of the time window and both edges of the pulse moved to compress or expand the width.
2. The lead edge can be held at the lead edge of the window and the tail edge modulated.
3. The tail edge can be fixed and the lead edge modulated.

3. OPTIMAL TORQUE RIPPLE AND SWITCHING SEQUENCE ANALYSIS:

The DTC-SVM driven motor torque ripple patterns depend on many factors such as stator flux amplitude, reference voltage amplitude, motor synchronous speed, etc. Conventionally, the definite prediction of the ripple pattern can only be done by detailed simulation of the whole system. This section introduces an insightful method to approach the torque ripple from a space vector perspective. With the methodology introduced, the torque ripple patterns can be analytically predicted and it is then possible to find the optimal switching sequence to realize the lowest torque ripple. Note that the same methodology can also be applied to the 3- phase system SVM torque analysis.

3.1. Stator Flux Rotation Speed and Amplitude Variation:

In ideal steady-state operation, the stator flux λ_s and rotor flux λ_r vectors both rotate at the electric synchronous speed ω_s , with λ_s leading λ_r by the angle δ . The instantaneous torque is expressed as:

$$T_e = K \cdot |\lambda_r| \cdot |\lambda_s| \cdot \sin(\delta) \quad 3.1$$

Where K is a coefficient depending on the motor parameters. In an inverter-fed motor drive, the rotor flux rotation can still be regarded as constant speed due to its large time constant. However, the speed and the amplitude of the λ_s depend on currently applied voltage vector. The following equations calculate the λ_s instantaneous rotation speed and amplitude variation when a certain voltage vector is applied:

$$\omega_{\lambda_s} = \frac{v_{x,tan-proj} \cdot D_x \cdot T_{DSP}}{D_x \cdot T_{DSP} \cdot |\lambda_s|} = \frac{v_{x,tan-proj}}{|\lambda_s|} \quad 3.2$$

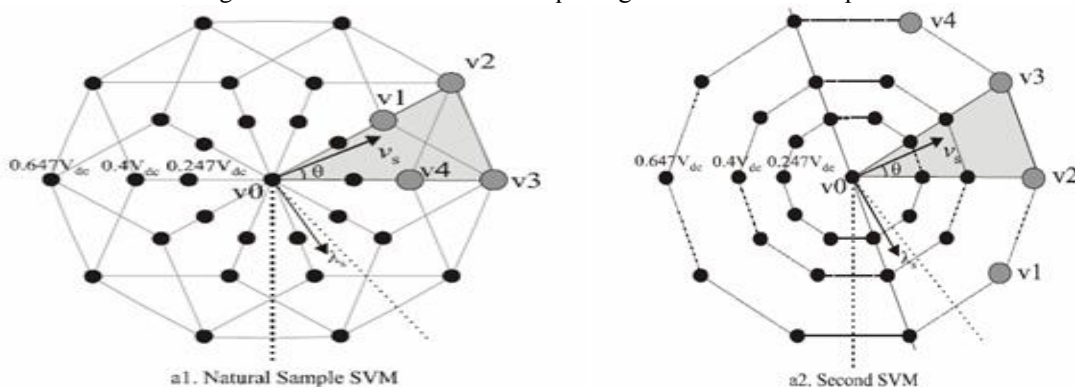
$$\Delta |\lambda_s| = v_{x,radial-proj} \cdot D_x \cdot T_{DSP} \quad 3.3$$

where $V_{x,tan-proj}$ and $V_{x,radial-proj}$ are the voltage vector tangential and radial projections along the λ_s locus; D_x is the duty ratio of the voltage vector; $V_{x,tan-proj} \cdot D_x$ and $V_{x,radial-proj} \cdot D_x \cdot T_{dsp}$ are the tangential/radial displacement of the stator flux with the voltage vector, which is then divided by vector active time $D_x \cdot T_{dsp}$ and the stator flux magnitude $|\lambda_s|$ to get the instantaneous angular speed.

The resulting ω_{λ_s} is either larger or smaller than ω_s (rotor flux speed). This changes the δ angle and the instantaneous torque fluctuates accordingly. Additionally, the $|\lambda_s|$ variation also affects the torque. As discussed next, the resulting torque ripple has different patterns depending on synchronous speed ω_s and the angular position of λ_s .

3.2. Torque Ripple Pattern Evolution and On-line Torque Slope Determination :

As shown in Figures 5.1a and 5.2a, the torque ripple is analyzed in the highlighted sector 1 for both SVM methods, and the results are applicable to all ten sectors. Assuming the resistive voltage drop in is negligible, the flux λ_s and the VSI reference voltage vector v_s are 90° apart. The angle θ is the angle between the v_s and the lower boundary of the sector. As flux angular position, or θ , increases within the sector, the tangential projections of four active vectors used in each PWM cycle (in larger grey dots) will change, hence their instantaneous stator flux rotating speed $\lambda_s \omega$. In Figures 5.1b and 5.2b, the $\lambda_s \omega$ for four vectors are plotted along $0^\circ < \theta < 36^\circ$ for both SVM methods. The horizontal dotted line represents the rotor flux speed ω_s , which is adjusted by the DTC control. Depending on the ω_s and the stator flux angular position θ , the ω_{λ_s} of each voltage vector could be either higher or lower than ω_s . The torque angle variation $\Delta\delta$ is expressed as follows



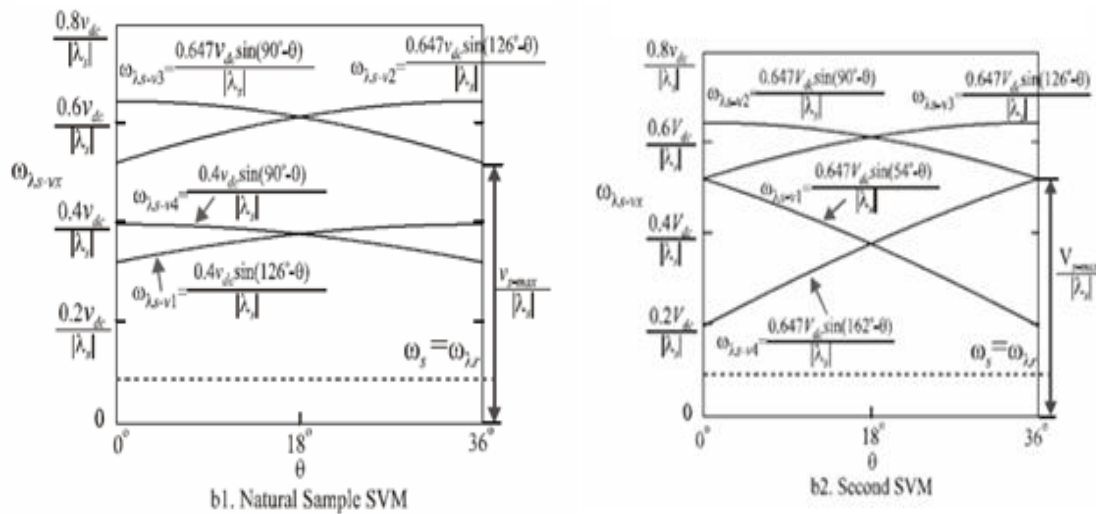


Figure 3.1 Torque ripple space vector analysis and its evolution over
3.2 different speed and stator flux angular position

To decide if the vector associated torque slope will be positive or negative, the $|\lambda_s|$ variation over the different angular position also needs to be considered. The set of curves similar to Figures 5b1 and 5b2. Obviously, for v_2 and v_3 , their $|\lambda_s| \omega - \omega$ value is much larger than that of the v_1 and v_4 . From 5.4, it is then concluded that the v_2 and v_3 will always create positive torque ramp and constitute the majority of torque increment in one PWM cycle.

The torque decrement occurs when zero vector is applied. The effects from v_1 and v_4 vectors can be ignored and regard as nearly “flat” torque ramps. The Figure 9 shows the zoom-in view of the torque ripple simulation when the motor speed is low and high (at no-load). The vector v_1 and v_4 torque slope evolve from positive to negative as motor speed increases. But their effects can be obviously ignored as previously concluded.

3.3. Simplified Prediction of Torque Pattern Evolution:

The above torque slope prediction method can be greatly simplified with following two facts. First, compared to torque angle variation, effects of the stator flux magnitude variation on the torque can be safely neglected; particularly at light load conditions (The proof of this fact is beyond the scope of the paper). So the torque slope direction for each vector can be directly found with Figures 3b1 and 3b2.

Secondly, for the total vectors cancellation in d2-q2 plane, the two pair of vectors has certain timing ratio between them. For example, in natural sample SVM, the timing ratio between v_2 and v_1 (or v_3 and v_4) is always 1.618:1. Therefore, the vector v_2 and v_3 has larger duty ratio than v_1 and v_4 .

The normal motor speed range is designated in Figures 3b1 and 53b2. Obviously, for v_2 and v_3 , their $|\lambda_s| \omega - \omega$ value is much larger than that of the v_1 and v_4 . From 5.4, it is then concluded that the v_2 and v_3 will always create positive torque ramp and constitute the majority of torque increment in one PWM cycle. The torque decrement occurs when zero vector is applied. The effects from v_1 and v_4 vectors can be ignored and regard as nearly “flat” torque ramps. The Figure 5.2 shows the zoom-in view of the torque ripple simulation when the motor speed is low and high (at no-load). The vector v_1 and v_4 torque slope evolve from positive to negative as motor speed increases. But their effects can be obviously ignored as previously concluded.

3.4. Optimal Vector Sequence:

The essence of the minimal torque ripple vector sequence is to reshuffle the order of the voltage vectors per DSP cycle to make the torque increase/decrease ramps sandwich each other. This way the maximum torque peak to peak value will only be equal to the largest torque variation with certain voltage vector, instead of the cascading of several ramps in the same direction.

However, the minimal torque ripple sequence might not have minimal numbers of switching per PWM cycle. For natural sampling SVM, the switching sequence is implicitly achieved by using the center-aligned triangular carrier. It has the lowest possible switching numbers (one per inverter state change). The vector sequence alternates between $(v_0(11111) - v_1 - v_3 - v_2 - v_4 - v_0(00000))$ and $(v_0(00000) - v_4 - v_2 - v_3 - v_1 - v_0(11111))$ as labeled in Figure 5.1. For the lowest switching loss, the switching sequence for the second SVM is as illustrated in Figure 10. Only one switching occurs at each switching state transition except for the one between the zero vector and vector 1 or 4.

Figure 3.3 only shows the sequence for the odd number sectors; for the even number sectors, the sequence from v1 to v4 is reversed. The switching sequence above will not give lowest torque ripple. With v1 and v4 ignored, the v2 and v3 are two cascaded torque increasing ramps. They can be separated by the zero-vector with certain duty ratio, which can be computed to achieve evenly distributed torque increasing and decreasing ramps, i.e. lowest torque ripple. This sequence reshuffling can be done on the fly for each DSP cycle and be easily integrated into the modulator. However, the increased control complexity and extra switching loss might be undesirable. For overall optimal vector sequence, the sequence with lowest switching number per cycle might still be preferred unless torque ripple performance is of higher priority in certain applications.

3.5. Further Comparison Between the two SVM Methods:

The second SVM method has four more switching events per DSP cycle than natural sampling SVM. Also it's more complicated to implement in a DSP. However, its d2-q2 plane PWM frequency harmonic current amplitude is slightly smaller, since all four vectors located along the outer ring in d1-q1 decagon are in the inner ring in the d2-q2 decagon. While both SVM methods produce zero average voltage/current in d2-q2, the PWM frequency current harmonics still exist and are proportional to the amplitudes of the d2-q2 voltage vectors used. By comparison, the natural sample SVM uses two mid-ring vectors in d2-q2 plane. Therefore higher PWM frequency harmonic currents exist.

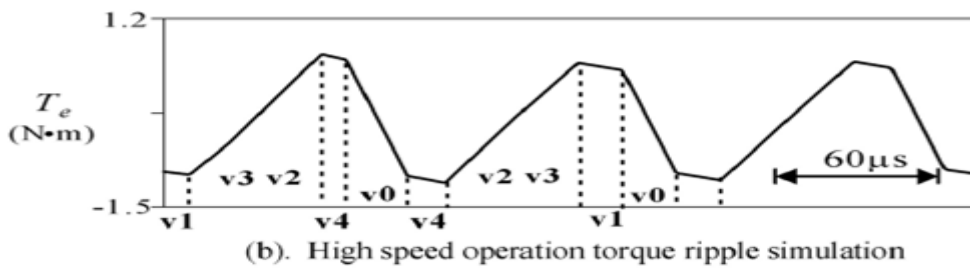
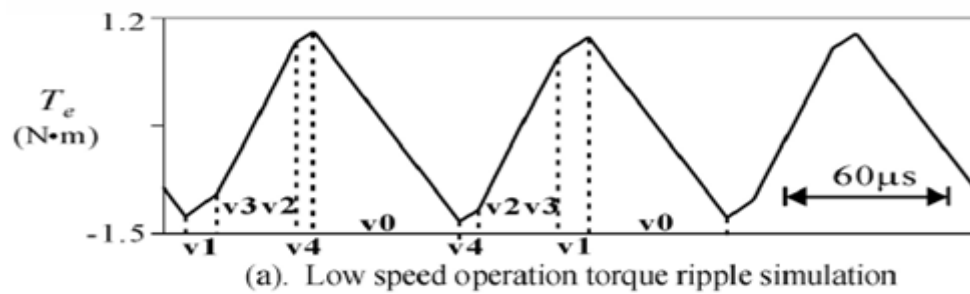


Figure 3.2 Natural sample SVM torque ripple pattern evolution over speed

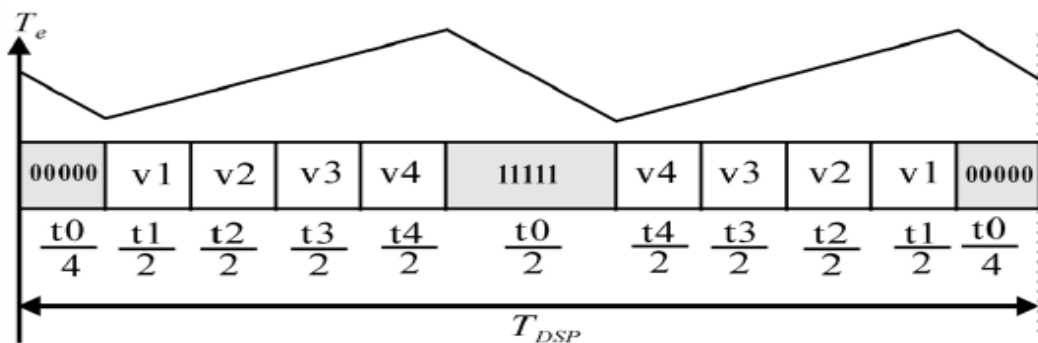


Figure 3.3 Optimal switching sequence and resulting torque ripple

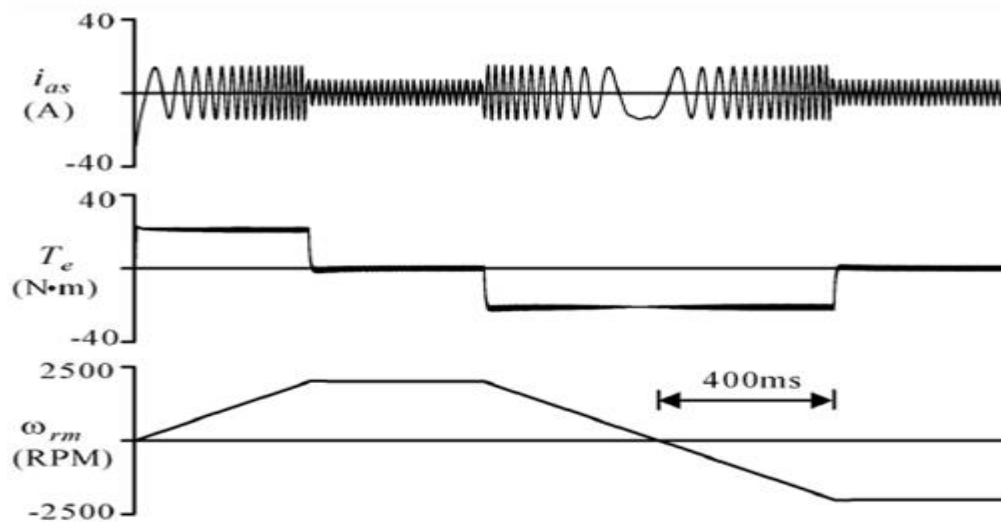


Figure 3.4 DTC-SVM simulation results(identical results for both SVMs)

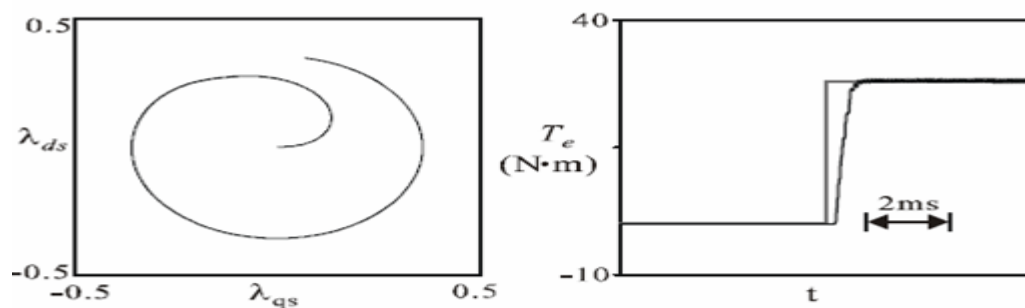
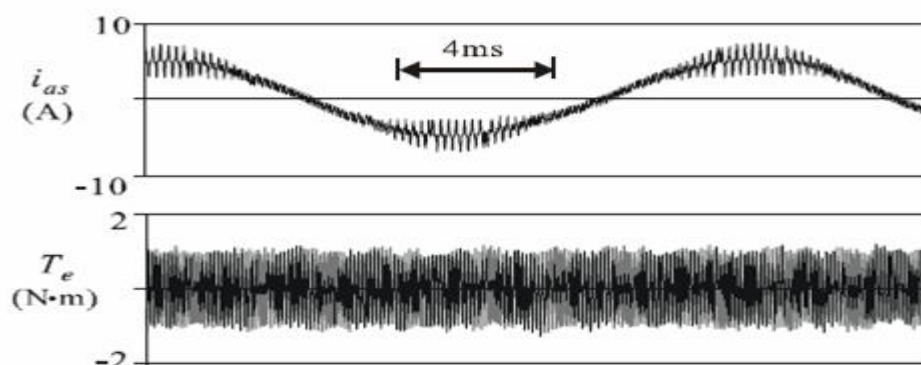
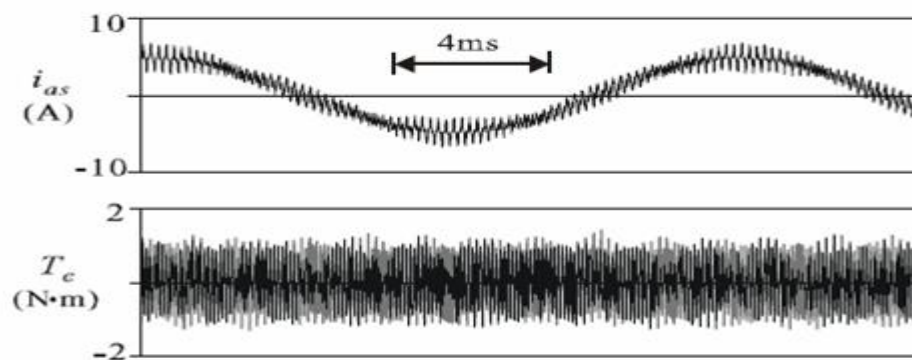


Figure 3.5 Start-up flux locus and torque step response



(a)SVM using four vectors along outer ring



(b) natural sampling SVM

Figure 3.6 Comparison of phase current and torque between and two schemes

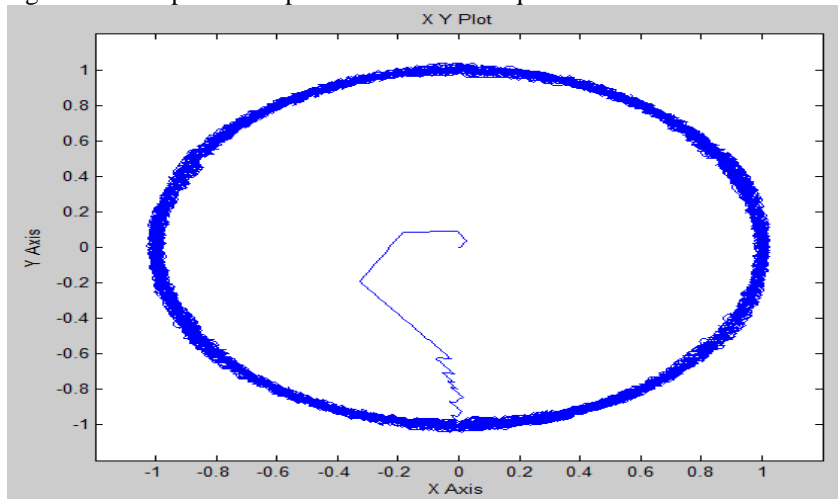


Figure 3.7 Air gap flux for simulation of five-phase induction motor

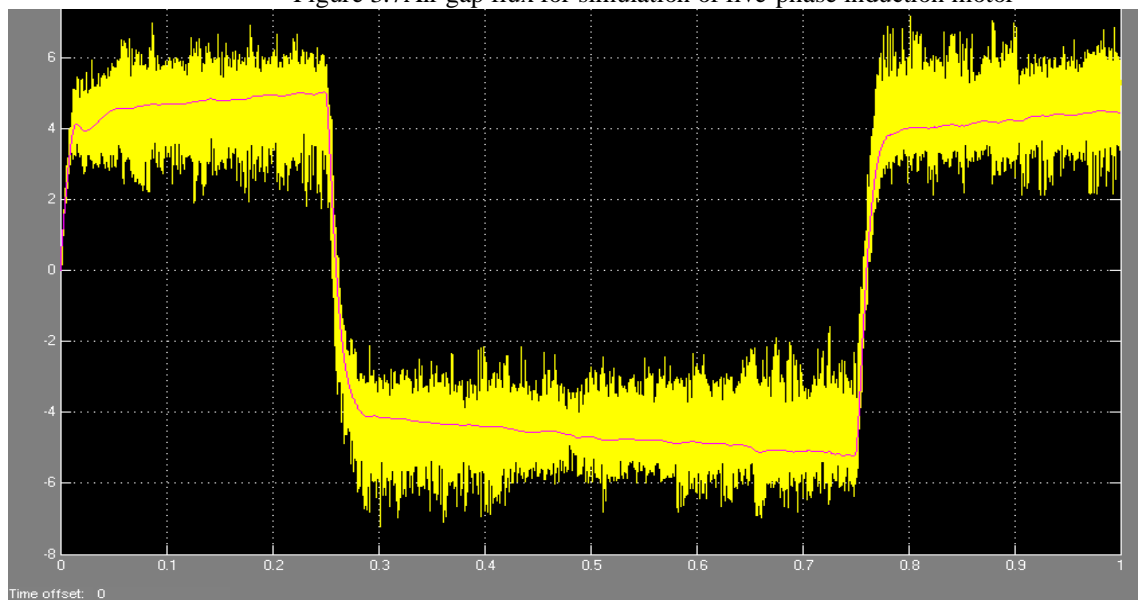


Figure 3.8 Normal torque

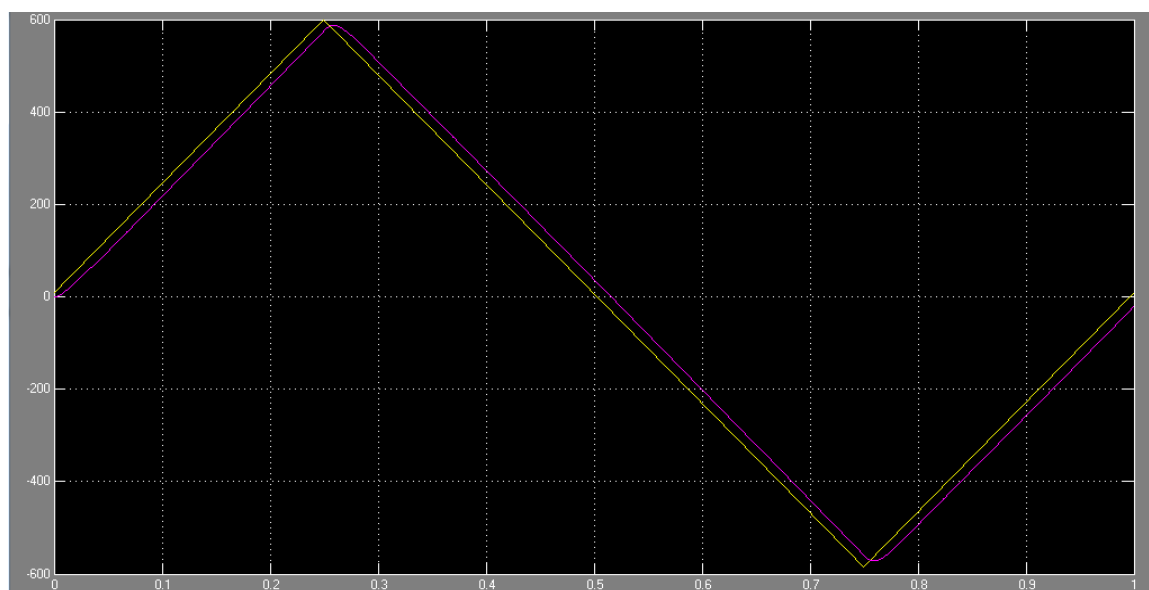


Figure 3.9 Comparison of normal speed and controlled speed

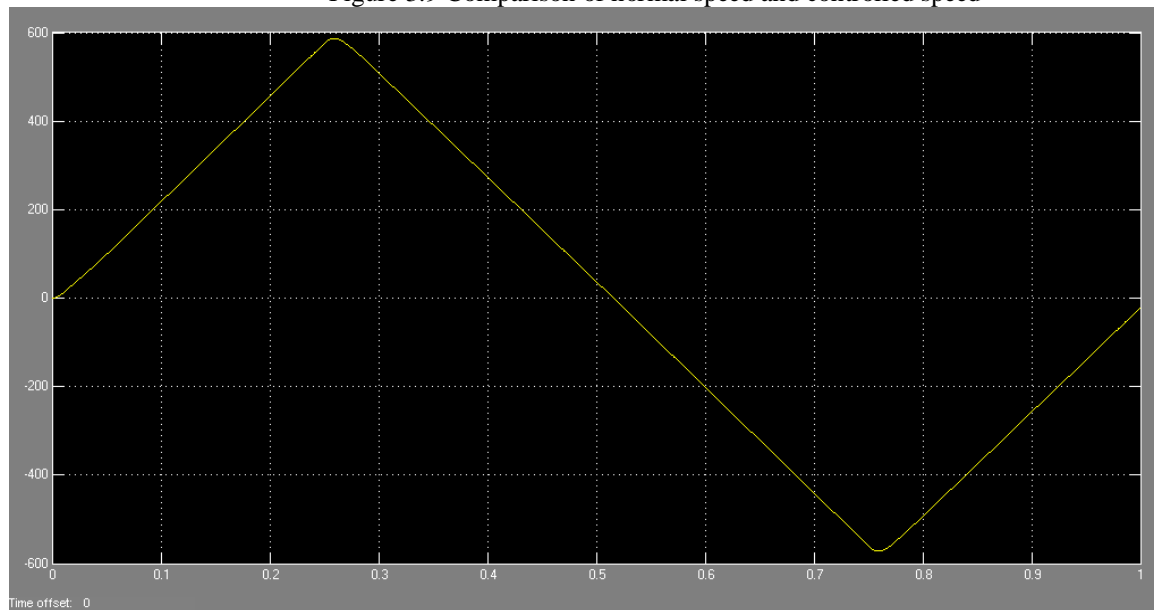


Figure 3.10 Controlled speed by DTC-SVM

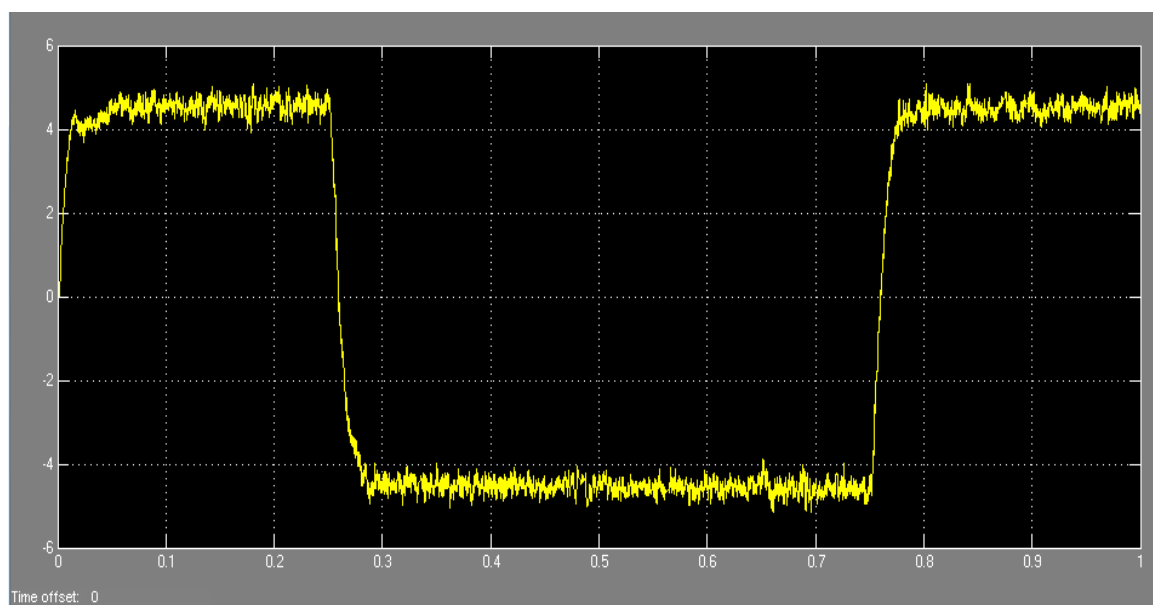


Figure 3.11 Torque produced by SVM

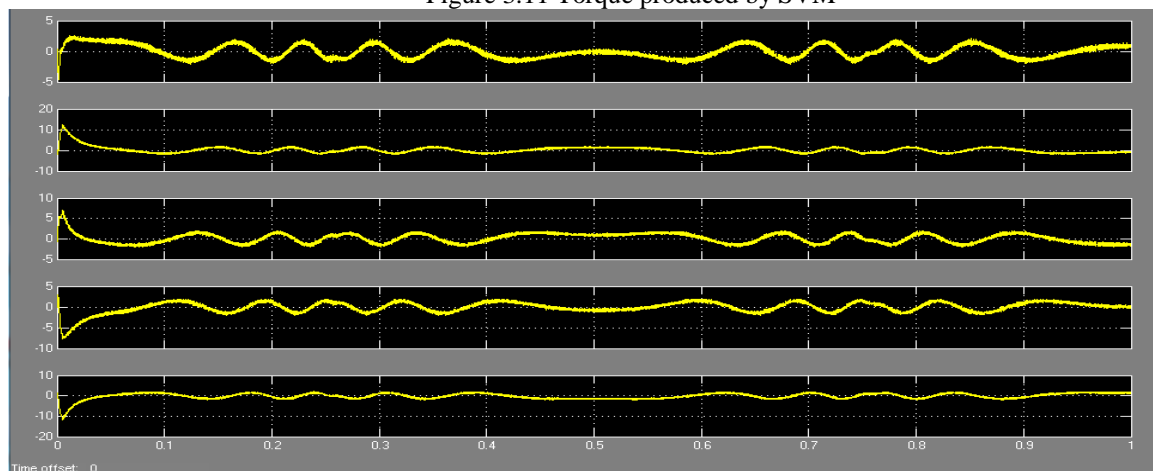


Figure 3.12 Stator currents of five-phase induction motor

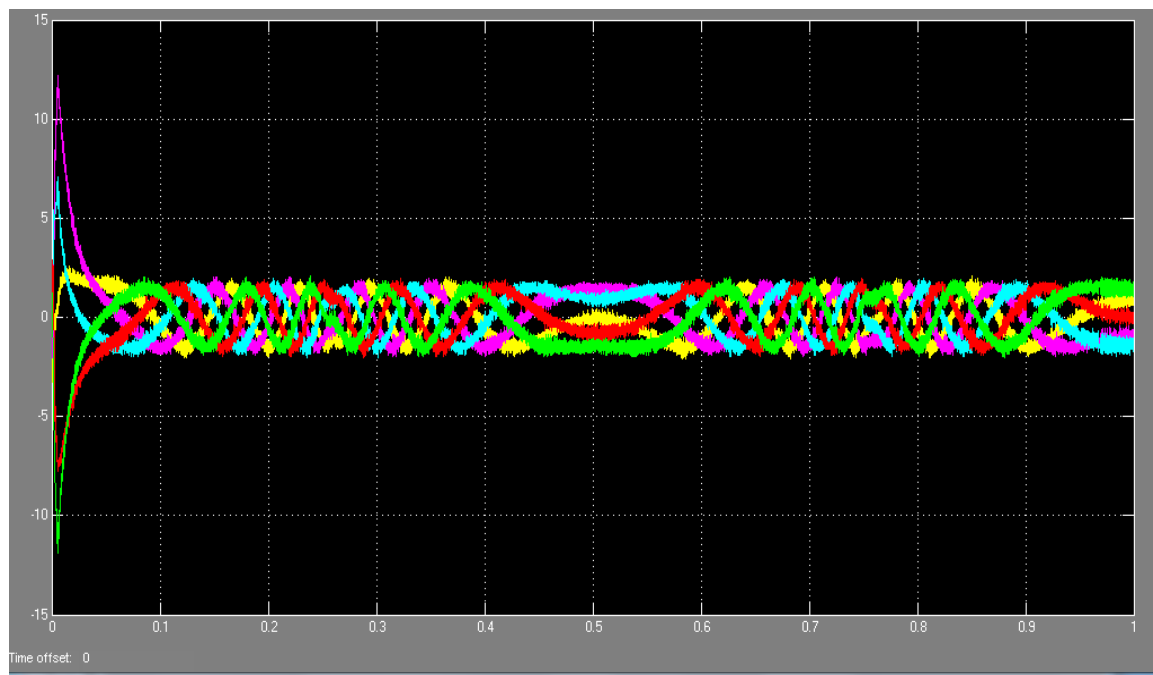


Figure 3.13 Torque produced in five-phase windings

In particular, flux build up locus during start-up and the step torque command response are shown. Figure 3.13 is the comparison of steady-state torque and phase current between the two SVM techniques. Except for the increase in PWM switching components in the natural sampling SVM, the results are similar. Both cases demonstrate sinusoidal waveforms without low frequency harmonics.

4. CONCLUSION:

The traditional lookup table direct torque control (DTC) in 5-phase induction motors with sinusoidal distributed windings suffers from two drawbacks. The first problem is the larger torque ripple when digital hysteresis implementation is used. The second is that the sinusoidal distributed windings in a 5-phase motor have no back-EMF for certain low frequency non-torque producing harmonics and these harmonic voltages can be introduced by the lookup table DTC method and create large harmonic currents. To address these issues, the conventional DTC-SVM is extended into a 5-phase system to improve the steady-state performance. Specifically, this paper introduced two SVM schemes to cancel out all possible low frequency voltage harmonics. To provide a complete set of solution, the optimal switching sequence is also analyzed. Based on the instantaneous stator flux angle and amplitude variation, the torque ripple pattern evolution and its relationship with the torque ripple reduction are studied in an insightful way. Detailed simulations verify the effectiveness of the DTC-SVM control both in dynamic and steady-state performance.

ACKNOWLEDGEMENTS

I Thank to our Institute Executive directors Mr.T Sai kumar & Mr.D Baba for providing creative environment for this work. Also I am very much thankful to our Institute principal Dr. K Ramesh for his kind permission and encouragement to write research paper. I would like to extend my heartfelt thanks to my colleagues. And finally I am very much obliged to my respected parents who inspiring me around the clock.

AUTHOR BIOGRAPHY



Jyothilal Nayak Bharothu received the B.E (Electrical &Electronics Engg.) from S.R.K.R Engg. College Bhimavaram (Andhra University) and M.Tech;(Power systems- High Voltage Engg) from JNTU KAKINADA University . He has six years of teaching experiences in the field of Electrical Engg. in India, his field of interest is power systems operation and control. He has published four papers in international Journals. Presently, he is Associate professor of EEE Dept at Sri Vasavi Institute of Engineering and Technology, Nandamuru, A.P, INDIA



V.Gopi Latha is currently working as an Assistant Professor in Electrical and Electronics Engineering Department, Sri Vasavi Institute of Engineering & Technology, Pedana, Andhra Pradesh, India. She received her B.Tech. degree in Electrical & Electronics Engineering from Swarnandhra College of Engineering & Technology affiliated to JNT University in 2006, Andhra Pradesh, India and the M.Tech. degree in Power Electronics from Nova College of Engineering & Technology, Jangareddy gudem, WGDIST, affiliated to JNTK University, Andhra Pradesh, India, in 2010.

References

- [1]. G.S. Buja and M.P. Kazmierkowski, "Direct torque control of PWM inverter-fed AC motors - a survey," IEEE Transactions on Industrial Electronics, volume 51, number 4, pages 744-757, August 2004
- [2]. I. Takahashi and Y. Ohmori, "High-performance direct torque control of induction motor," IEEE Transactions on Industrial Applications, volume 25, number 2, pages 257-264, 1989.
- [3]. X. Xue, X. Xu, T.G. Habetler, and D.M. Divan, "A low cost stator flux oriented voltage source variable speed drive," Proceeding of the IEEE Industry Applications Society Conference, volume 1, pages 410-415, 1990.
- [4]. T.G. Habetler, F. Profumo, M. Pastorelli, and L.M. Tolbert, "Direct torque control of induction motor using space vector modulation," IEEE Transactions on Industrial Applications, volume 28, pages 1045-1053, September/October 1992.
- [5]. Y.S. Lai and J.H. Chen, "A new approach to direct torque control of induction motor drives for constant inverter switching frequency and torque ripple reduction," IEEE Transactions on Energy Conversion, volume 16, number 3, pages 220-227, September 2001.
- [6]. H.A. Toliyat and H. Xu, "A novel direct torque control (DTC) method for five-phase induction machines," Proceedings of the IEEE Applied Power Electronics Conference, volume 1, pages 162-168, September 2001.
- [7]. L. Parsa and H.A. Toliyat, "Five-Phase Permanent-Magnet Motor Drives," IEEE Transactions on Industry Applications, volume 41, number 1, pages 30-37, January/February 2005.
- [8]. H.A. Toliyat, "Analysis And Simulation of Five-Phase Variable-Speed Induction Motor Drives Under Asymmetrical Connections," IEEE Transactions on Power Electronics, volume 13, number 4, pages 748- 756, July 1998.
- [9]. Y. Zhao and T.A. Lipo, "Space Vector PWM Control of Dual Three Phase Induction Machine Using Vector Space Decomposition," IEEE Transactions on Industry Applications, volume 31, number 5, pages 1100-1109, 1995.
- [10]. K.N. Pavithran, R. Parimelalagan, and M.R. Krishnamurthy, "Studies on Inverter-Fed Five-Phase Induction Motor Drive," IEEE Transactions on Power Electronics, volume 3, number 2, pages 224-235, 1988.
- [11]. S. Lu and K.A. Corzine, "Multilevel multi-phase propulsion drives," Proceedings of the IEEE Electric Ship Technologies Symposium, pages 363-370, July 2005.